JOC The Journal of Organic Chemistry

Article

pubs.acs.org/joc

Modular Synthesis of Aromatic Hydrocarbon Macrocycles for Simplified, Single-Layer Organic Light-Emitting Devices

Koki Ikemoto,[†,‡] Asami Yoshii,[§] Tomoo Izumi,[†,∥] Hideo Taka,[†,∥] Hiroshi Kita,[∥] Jing Yang Xue,[§] Ryo Kobayashi,[§] Sota Sato,*[,†,‡,§] and Hiroyuki Isobe*[,†,‡,§]

[†]JST, ERATO, Isobe Degenerate π-Integration Project, Aoba-ku, Sendai 980-8577, Japan

[‡]Advanced Institute for Materials Research and [§]Department of Chemistry, Tohoku University, Aoba-ku, Sendai 980-8577, Japan

[∥]Konica Minolta, Ishikawa-cho, Hachioji 192-8505, Japan

Supporting Information

ABSTRACT: A method for the modular synthesis of aromatic hydrocarbon macrocycles has been developed for base materials in single-layer organic light-emitting devices. The method with Ir-catalyzed direct C−H borylation and Suzuki−Miyaura coupling was concise and scalable, which allowed for a gram-scale preparation of aromatic hydrocarbon macrocycles that have bulky substituents at the periphery. The new arylated hydrocarbon macrocycles enabled a quantitative electro-optical conversion in organic light-emitting devices with a phosphorescent emitter, which is, notably, in a single-layer architecture consisting of two regions of doped and undoped materials. The highest external quantum efficiencies reached 24.8%, surpassing those of previous hydrocarbon base materials.

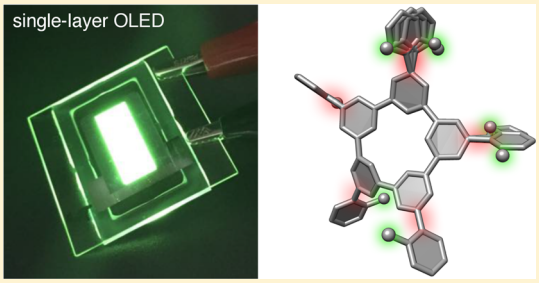

INTRODUCTION

Possessing conjugated π-electrons, aromatic structures comprise the most important structural motif in organic electronics. Although the most primary aromatic structure, an aromatic hydrocarbon, was favorably utilized for segments of electronic molecular materials in combinations with other elements, the macrocyclization of aromatic hydrocarbons was recently found effective for designing unique organic electronic materials especially for organic light-emitting devices (OLEDs).[1−4] The intrinsic bipolar charge carrier transport abilities of naphthalene[5] or benzene[6] were thus integrated into both hole-transport-layer and electron-transport-layer materials of OLEDs through the one-pot macrocyclization of the primary hydrocarbon units without recruiting other elements.[1,2] Recent examples of methylated [*n*]cyclo-*meta*-phenylene ([*n*]CMP,[2] Scheme 1) revealed the unexpected yet remarkable importance of steric design at the periphery of the macrocycles. The two-role, bipolar transport functions of unsubstituted [*n*]CMP further evolved, upon methylation at the periphery, into multirole base materials that played all the requisite functions for delivering charge carriers and resultant energies to the phosphorescent emitter. A phosphorescent, three-region single-layer OLED with a highly efficient electro-optical conversion was thus generated with a single-component hydrocarbon macrocycle, *n*Me-[*n*]CMP (Scheme 1),[7] and the design principle of the base materials in emerging single-layer OLEDs has departed from the elaborate, multiple-component design using heteroatoms.[8,9] Although the one-pot macrocyclization method in the previous studies fulfilled a synthetic conciseness necessary for preparations of prototype macrocycle materials, the synthesis of a variety of substituted [*n*]CMP hydrocarbons for further exploration is not readily feasible: the one-pot macrocyclization method inevitably requires dihalogenated benzene derivatives as the monomeric precursor that, by itself, requires synthetic efforts and investigations (Scheme 1).[2,7] In this study, we have exploited a novel modular synthesis route for the substituted hydrocarbon congeners of [*n*]CMP and, consequently, developed a unique molecular material that enabled simplified architectures in the

Scheme 1. Two Synthesis Routes for [*n*]CMP Derivatives

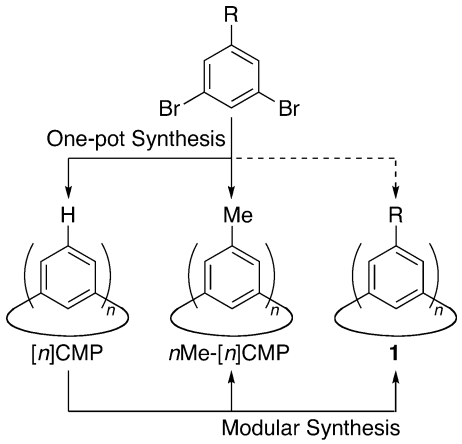

Received: November 15, 2015
Published: December 11, 2015

DOI: 10.1021/acs.joc.5b02620
J. Org. Chem. 2016, 81, 662−666

high-performance single-layer OLED. We found that the Ir-catalyzed direct borylation reaction of [*n*]CMP proceeds selectively at desirable positions in a nearly quantitative manner, which allowed us to introduce bulky substituents at the periphery through subsequent Suzuki–Miyaura coupling reactions. With the modular synthesis enabling the large-scale preparation of arylated [*n*]CMP **1**, we obtained single-layer OLEDs with the highest level of electro-optical conversion in a two-region architecture. The steric design of aromatic hydrocarbon macrocycles may flourish through the modular synthesis methods for high-performance, single-layer OLEDs.

RESULTS AND DISCUSSION

The modular synthesis for introducing substituents in [*n*]CMP was concise and versatile, starting from Ir-catalyzed direct C–H borylation.[10,11] After preparation of the precursor macrocycle, [*n*]CMP (*n* = 5 and 6), in gram quantities from one batch of our Ni-mediated macrocylization,[2] we examined the direct borylation reaction by using $[Ir(cod)(OMe)]_2$ and dtbpy (Scheme 2). When we first examined conventional conditions while

Scheme 2. Modular Synthesis of Substituted [*n*]CMP

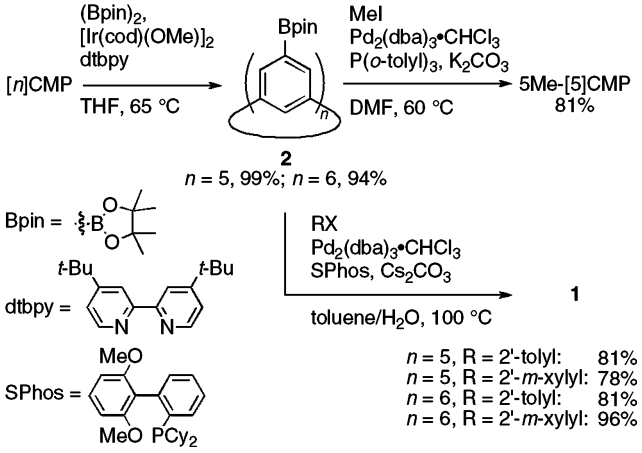

adopting cyclohexane as the solvent, the reaction did not proceed to completion, even under high-temperature conditions. Then, we changed the solvent to THF and found it suitable for the reaction: [*n*]CMP borylation proceeded in THF, providing fully borylated macrocycles **2** in excellent yields (99% yield for *n* = 5 and 94% yield for *n* = 6). The method was concise and scalable, and both of the borylated [*n*]CMP macrocycles (*n* = 5 and 6) were obtained in gram quantities from a single batch without recourse to the column chromatography for purification.

The Suzuki–Miyaura coupling reactions furnished the [*n*]CMP macrocycles with substituents at the periphery.[12] First, we describe the methylation of [5]CMP with iodomethane. The five-fold coupling reaction of [5]CMP proceeded smoothly with iodomethane in the presence of a catalytic amount of $Pd_2(dba)_3{\cdot}CHCl_3$ to afford 5Me-[5]CMP in 81% yield (Scheme 2). The yields of [5]CMP and 5Me-[5]CMP with the previous one-pot macrocyclization were 17 and 15%, respectively,[2,7] and by recording the total value of 14%, the yield of 5Me-[5]CMP by a three-step synthesis via the present modular route was comparable to that of one-pot synthesis.

We next describe arylation of [*n*]CMP. The arylation of [*n*]CMP (*n* = 5 and 6) was performed with the same Pd catalyst under slightly modified conditions. Considering the importance of the steric bulkiness of the substituents for the multirole base materials in single-layer OLEDs (vide infra),[7] we adopted 2-bromotoluene and 2-bromo-*m*-xylene as the 2′-tolyl and 2′-*m*-xylyl donors for the coupling reactions with **2**. The arylated [5]CMPs (**1**) were obtained in 81 and 78% yields for the 2′-tolyl and 2′-*m*-xylyl substituents, respectively, and the arylated [6]CMPs (**1**) were likewise obtained in 81 and 96% yields for the 2′-tolyl and 2′-*m*-xylyl substituents, respectively.

The molecular structures of new arylated [*n*]CMPs in the crystalline solid state were revealed by X-ray crystallographic analyses. As was the case with previous methylated congeners,[2,7] the arylated [5]CMPs with odd-numbered phenylene units possessed nonsymmetric environments on each side of the macrocyclic opening, whereas the arylated [6]CMPs possessed symmetric environments on both sides. For instance, as shown for the structures with the mean plane of macrocyclic opening in Figure 1, three hydrogen atoms in the opening of [5]CMP were

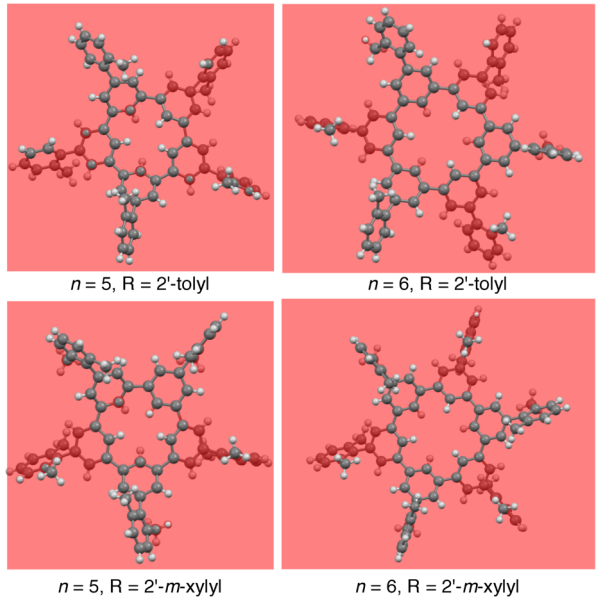

Figure 1. Crystal structures of **1**. In the crystal, several molecules with similar structures are located as disordered or nonequivalent structures, and one representative structure is shown for each molecule. The mean planes of the carbon atoms at the macrocyclic opening are drawn in red using Mercury CSD software (CCDC, v.3.6), and molecules are viewed perpendicular to the plane.

located above the plane, and two other hydrogen atoms were located on the opposite side. The hydrogen atoms of [6]CMP were evenly distributed on each side as a result of the alternate arrangement of the phenylene units. The structural difference between the 2′-tolyl and 2′-*m*-xylyl substituents did not affect the overall macrocyclic structures, and the aryl substituents were commonly perpendicular to the phenylene unit of the macrocycles. Further details of the molecular structures are discussed below in association with the device performance.

Using the arylated [*n*]CMP macrocycles, the device architectures of single-layer OLEDs could further be simplified without risking electro-optical conversion. The fundamental properties that are important for the device characteristics are first described in comparison with the methylated congeners (Table 1). The aryl substituents supported the thermal stability of macrocycles and increased the decomposition temperature (T_d). As shown in Table 1, the 2′-tolyl and 2′-*m*-xylyl

DOI: 10.1021/acs.joc.5b02620
J. Org. Chem. 2016, 81, 662–666

Table 1. Fundamental Properties of [*n*]CMP

[*n*]CMP	T_d (°C)[a]	λ_{max} (nm)[b]	HOMO (eV)[c]	LUMO (eV)[c]
5Me-[5]CMP	369[d]	256[d]	−5.77	−0.95
1 (*n* = 5, R = 2′-tolyl)	476	257	−5.95	−1.17
1 (*n* = 5, R = 2′-*m*-xylyl)	463	256	−6.00	−1.23
6Me-[6]CMP	433[d]	255[d]	−5.71	−0.94
1 (*n* = 6, R = 2′-tolyl)	509	258	−5.91	−1.14
1 (*n* = 6, R = 2′-*m*-xylyl)	518	255	−5.96	−1.21

[a]The onset decomposition temperature in helium. [b]UV−vis absorption maximum in $CHCl_3$. [c]DFT calculations with B3LYP/6-31G(d,p). [d]Data from ref 7.

substituents increased the T_d values by +107 °C at the maximum and increased all of the T_d values above 450 °C. The absorption spectra demonstrated that the transparency of the macrocycles in the visible light region was maintained with absorption maxima that were located at approximately 260 nm. The theoretical calculations with the DFT method [B3LYP/6-31G(d,p)] revealed the subtle electronic effects of aryl substituents as follows: both HOMO and LUMO energy levels were slightly lowered, and the resultant energy levels did not deviate substantially among the arylated congeners.

The device performances are described next. In our previous study,[7] we adopted a single-layer architecture consisting of three regions, as is often the case with preceding examples with multicomponent materials.[8,9] In the previous three-region single-layer architecture, a region doped with a phosphorescent emitter of $Ir(ppy)_3$ was sandwiched between undoped regions of the base materials in a three-region configuration of anode/undoped region (10 nm)/doped region (40 nm; 6 wt % $Ir(ppy)_3$)/undoped region (10 nm)/cathode. In this study, we found that the architectures of the single-layer OLEDs can be further simplified into two-region devices with aromatic hydrocarbon materials. Considering the peculiar effect of 5Me-[5]CMP in retarding the hole mobility of the single-layer OLED,[7] we postulated that the undoped region on the electron transport side could readily be eliminated. A simplified, two-region device with a configuration of anode/undoped region (10 nm)/doped region (60 nm; 6 wt % $Ir(ppy)_3$)/cathode was thus fabricated, and its performance was evaluated in terms of the external quantum efficiency (EQE), driving voltage (DV), power efficiency (PE), and current efficiency (CE) at 0.1 mA·cm^{-2} (Table 2).[13] The performances of the methylated congeners, *n*Me-[*n*]CMPs, were similar to those observed with the three-region devices, demonstrating the feasibility of two-region single-layer OLEDs with aromatic hydrocarbon macrocycles. The methylated congener, 5Me-[5]CMP, had the utmost level of electro-optical conversion with a corresponding EQE value of 21.4%, and 6Me-[6]CMP was much less effective as the base material.[7]

Table 2. Device Performance of the Two-Region Single-Layer OLED[a]

base material	EQE (%)	DV (V)	PE (lm·W^{-1})	CE (cd·A^{-1})
5Me-[5]CMP	21.4	5.9	40.1	75.4
6Me-[6]CMP	8.5	4.7	20.5	30.8
1 (*n* = 5, R = 2′-tolyl)	24.8	5.1	54.4	88.0
1 (*n* = 5, R = 2′-*m*-xylyl)	18.7	5.8	36.0	67.3
1 (*n* = 6, R = 2′-tolyl)	14.2	5.5	28.6	50.1
1 (*n* = 6, R = 2′-*m*-xylyl)	14.6	6.3	26.0	51.8

[a]The device performances were evaluated at a constant current of 0.1 mA·cm^{-2} in the two-region device configurations of anode/undoped region (10 nm)/doped region (60 nm, 6 wt % of $Ir(ppy)_3$)/cathode. The anode was fabricated with ITO (110 nm)/PEDOT:PSS (30 nm), and the cathode was fabricated with Cs (1.5 nm)/Al (100 nm).

We were delighted to observe that the arylated congener showed the highest, superior performances in the two-region architecture. Thus, the highest EQE value (24.8%) as well as the best values for the PE (54.4 lm·W^{-1}) and CE (88.0 cd·A^{-1}) was recorded with the 2′-tolylated [5]CMP congener. Because the light generated in the device cannot be fully emitted outside, limiting the highest reachable EQE values to 20−30%, even with 100% electro-optical conversion,[14] the EQE value of 24.8% with the 2′-tolylated [5]CMP originates from the 100−83% electro-optical conversion in the device. Albeit less effective, all the other arylated congeners also showed high EQE values (above 10%), which has rarely been achieved for three-region single-layer OLEDs with multicomponent (donor−acceptor) base materials that contain heteroatoms in elaborate structures.[8,9]

Considering the device characteristics in conjunction with the detailed examinations of the molecular structures, we suggest the following description for the device performance origin. The high performance of the two-region single-layer OLEDs with the EQE values over 10% indicates the appropriateness of all arylated [*n*]CMP hydrocarbons as multirole base materials. The steric design at the periphery should be essential to insulate the phenylene units in the macrocycles from the direct intermolecular contacts in the solid thin films.[7] As a result, the intrinsic high-energy level of the excited triplet state of [*n*]CMPs can be maintained in the thin film, which facilitates the efficient phosphorescence from the emitter. The hindrance effects of aryl groups were particularly effective for helping [6]CMP congeners acquire the requisite characteristics for the base material. Considering the negligible differences in the electronic characters (vide supra), we conclude that the subtle differences in the performances among the arylated [*n*]CMP hydrocarbons likely also have steric origins. Among several steric differences in the arylated congeners, there is a subtle yet important difference in the locations of the methyl groups on the aryl substituents. Thus, when we overlaid the phenylene units of the observed crystal structures (Figure 2),[15] the methyl groups of the aryl substituents were evenly distributed on each side of the macrocycle, with the exception of the for 2′-tolyl substituents. Because of this, the two sides of the 2′-tolylated [5]CMP macrocyclic structure were nonsymmetrically covered with methyl groups in the crystal. Such biased locations are also likely present in the stochastic distributions in the thin films and, as a result, may favorably facilitate heterogeneous intermolecular contacts with the phosphorescent emitter. The heterogeneous intermolecular contacts should facilitate efficient hole transfer from the base material to the emitter, enabling the quantitative electro-optical conversion in simplified single-layer OLEDs.[7]

CONCLUSION

We have developed a modular synthesis method preparing phenylene macrocycles with bulky substituents at the periphery. The method with direct borylation and Suzuki−Miyaura coupling was concise and scalable, allowing us to screen substituted [*n*]CMP hydrocarbons for exploration of simplified single-layer OLEDs. All of the new [*n*]CMP hydrocarbons, with bulky aryl substituents, functioned remarkably well as the base materials in the two-region single-layer OLED, resulting in EQE

DOI: 10.1021/acs.joc.5b02620
J. Org. Chem. 2016, 81, 662−666

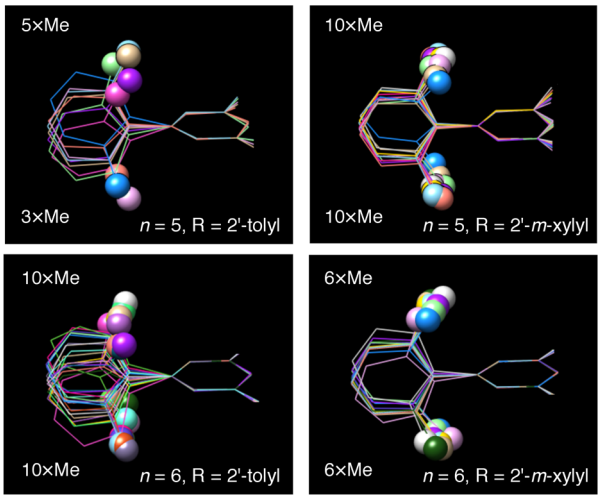

Figure 2. Overlaid structures of **1**. All phenylene units found in the crystal structures were overlaid and shown in different colors. The methyl groups on the aryl substituents are shown in ball models. The number of overlaid structures is as follows: 8 for n = 5, R = 2′-tolyl; 10 for n = 5, R = 2′-*m*-xylyl; 20 for n = 6, R = 2′-tolyl; and 12 for n = 6, R = 2′-*m*-xylyl.

values above 10%. These observations confirmed the importance of the steric design at the periphery of the macrocycles. The 2′-tolylated [5]CMP had the best and quantitative electro-optical conversion in the two-region device, with the utmost EQE values of 24.8%. The device performance achieved with 2′-tolylated [5]CMP indicated the importance of unevenly located substituents. The emerging, simple architecture of the single-layer OLED should be fully exploited by designing novel molecules that solely consist of hydrogen and carbon atoms, which may in turn have practical use in the future.

EXPERIMENTAL SECTION

General. Analytical thin-layer chromatography (TLC) was performed on a glass plate coated with silica gel (0.25 mm thickness) containing a fluorescent indicator. Flash silica gel column chromatography was performed on silica gel 60N (spherical and neutral gel, 40–50 μm). Gel permeation chromatography (GPC) was performed with UV and RI detectors using 1H-40, 2H-40, and 2.5H-40 columns (eluent: $CHCl_3$). ^1H and ^{13}C nuclear magnetic resonance (NMR) spectra were recorded, and chemical shift values are given with respect to internal $CHCl_3$ for ^1H NMR (δ 7.26) and $CDCl_3$ for ^{13}C NMR (δ 77.16). Melting points were measured and were uncorrected. Infrared (IR) spectroscopy was reported in cm^{-1}. The final products were analyzed by high-pressure liquid chromatography (HPLC) with UV and RI detectors using Cosmosil Cholester (4.6 mm i.d. × 250 mm) and Cosmosil BuckyPrep (4.6 mm i.d. × 250 mm) at the flow rate of 1.0 mL/min at 40 °C in a column oven under the UV detection at 250 nm wavelength (eluent: $CHCl_3$/MeOH = 3:2) (Figure S1). Thermogravimetry differential thermal analysis (TG-DTA) was recorded as follows (Figure S2): the samples were first equilibrated to 40 °C for 10 min and then heated at a constant rate of 10 °C/min in flowing helium. Ultraviolet–visible (UV) spectroscopy was carried, and the spectra are shown in Figure S3. High-resolution mass spectra were performed using MALDI, DART, or APCI methods. Elemental analyses were performed for CHNCl elements. X-ray diffraction analyses of single crystals were carried out with a pixel array detector using multilayer mirror monochromated Cu Kα radiation. CrystalClear[16] was used for the data collection and processing. The structures were solved by the direct method with SIR program[17] or SUPERFLIP[18] and refined by full-matrix least-squares methods using the SHELXL program suite[19] running on the Rigaku CrystalStructure software program[20] or the Yadokari-XG 2009 software program.[21]

Solvents and reagents were purchased and used without any further purification unless otherwise noted. Anhydrous THF (stabilizer-free) and toluene were purified by a solvent purification system equipped with columns of activated alumina and supported copper catalyst. Ultrapure water was used for reactions and degassed prior to use. The macrocyclic precursors were prepared by a method reported in the literature.[2]

Typical Procedure of Borylation. A mixture of [5]CMP (1.01 g, 2.65 mmol), bis(pinacolato)diboron (6.67 g, 26.3 mmol), bis(1,5-cyclooctadiene)di-μ-methoxydiiridium(I) (873 mg, 1.32 mmol), and 4,4′-di-*tert*-butyl-2,2′-dipyridyl (dtbpy; 710 mg, 2.65 mmol) in THF (26.2 mL) was stirred at 65 °C for 24 h. After the mixture was cooled to ambient temperature, solvent was removed in vacuo. The residue was suspended in MeOH (100 mL) and filtered. Without further purification, **2** (n = 5) was obtained as an analytically pure form as a white powder (2.64 g, 99%).

***2** (n = 5):* mp >250 °C (not detected); T_d (onset) 459 °C (in helium atmosphere); IR (powder) 2978 (w), 1592 (w), 1410 (w), 1350 (s), 1304 (w), 1256 (m), 1146 (s), 996 (m), 896 (w), 874 (w), 851 (m), 756 (w), 715 (w), 670 (m), 651 (w) cm^{-1}; ^1H NMR (400 MHz, $CDCl_3$) δ 8.58 (t, J = 2.0 Hz, 5H), 8.26 (d, J = 2.0 Hz, 10H), 1.42 (s, 60H); ^{13}C NMR (100 MHz, $CDCl_3$) δ 140.6, 137.2, 130.8, 84.1, 25.1 (a signal for the carbon nuclei bonded to the boron nuclei was not observed due to the quadrupolar relaxation induced by the boron nuclei); HRMS (MALDI/FT ICR) m/z $[M + H]^+$ calcd for $C_{60}H_{76}B_5O_{10}$ 1009.5856, found 1009.5857. Anal. Calcd for $C_{60}H_{75}B_5O_{10}$: C, 71.33; H, 7.48. Found: C, 70.99; H, 7.48.

***2** (n = 6).* 94% yield (3.76 g); mp >250 °C (not detected); T_d (onset) 477 °C (helium atmosphere); IR (powder) 2978 (w), 1409 (m), 1361 (s), 1315 (m), 1284 (m), 1268 (m), 1143 (s), 967 (m), 898 (w), 850 (s), 716 (s), 670 (m), 645 (m) cm^{-1}; ^1H NMR (600 MHz, $CDCl_3$) δ 8.31 (t, J = 1.8 Hz, 6H), 8.23 (d, J = 1.8 Hz, 12H), 1.44 (s, 72H); ^{13}C NMR (150 MHz, $CDCl_3$) δ 140.9, 132.4, 130.3, 84.2, 25.1 (a signal for the carbon nuclei bonded to the boron nuclei was not observed due to the quadrupolar relaxation induced by the boron nuclei); HRMS (APCI/TOF) m/z $[M + H]^+$ calcd for $C_{72}H_{91}B_6O_{12}$ 1213.7116, found 1213.7100. Anal. Calcd for $C_{72}H_{90}B_6O_{12}$: C, 71.33; H, 7.48. Found: C, 71.80; H, 7.57.

Typical Procedure of Methylation. To a mixture of tris(dibenzylideneacetone)dipalladium(0) chloroform adduct (25.9 mg, 0.025 mmol) and tri(*o*-tolyl)phosphine (30.4 mg, 0.10 mmol) in DMF (1.0 mL) were added borylated [5]CMP **2** (50.5 mg, 0.050 mmol) and K_2CO_3 (69.1 mg, 0.50 mmol). The mixture was heated at 60 °C, and methyl iodide (20.2 μL, 0.325 mmol) was added dropwise. The mixture was stirred at 60 °C for 24 h and was diluted with water (10 mL). After extraction with CH_2Cl_2 (10 mL × 3), the combined organic layer was dried on Na_2SO_4 and the solvent was removed in vacuo. The residue was purified by silica gel chromatography (eluent: $CHCl_3$/hexane = 1:4) and GPC to afford 5Me-[5]CMP as a white powder (18.8 mg, 81%). The spectroscopic data of the product matched those of 5Me-[5]CMP as reported previously.[7]

Typical Procedure of Arylation. To a mixture of tris(dibenzylideneacetone)dipalladium(0) chloroform adduct (154 mg, 0.149 mmol) and 2-dicyclohexylphosphino-2′,6′-dimethoxybiphenyl (127 mg, 0.309 mmol) in toluene (10 mL) were added borylated [5]CMP **2** (1.50 g, 1.48 mmol), 2-bromotoluene (3.6 mL, 29.9 mmol), toluene (20 mL), and 1 M aqueous solution (15 mL) of Cs_2CO_3 (4.89 g, 15.0 mmol). The mixture was vigorously stirred at 100 °C for 24 h and was diluted with water (100 mL). After extraction with CH_2Cl_2 (100 mL × 3), the combined organic layer was dried on Na_2SO_4, and the solvent was removed in vacuo. The residue was washed with hexane (50 mL) and purified by silica gel column chromatography (eluent: toluene) and GPC. The macrocyle **1** (n = 5, R = 2′-tolyl) was obtained as a white powder (1.01 g, 81%).

***1** (n = 5, R = 2′-tolyl):* mp >250 °C (not detected); T_d (onset) 476 °C (helium atmosphere); IR (powder) 3053 (w), 1579 (w), 1489 (w), 1453 (w), 1388 (w), 1324 (w), 1115 (w), 1034 (w), 868 (m), 765 (s), 728 (m), 713 (m), 680 (w), 627 (m) cm^{-1}; ^1H NMR (400 MHz, $CDCl_3$) δ 8.68 (t, J = 1.6 Hz, 5H), 7.71 (d, J = 1.6 Hz, 10H), 7.37–7.27 (m, 20H), 2.37 (s, 15H); ^{13}C NMR (100 MHz, $CDCl_3$) δ 143.2, 142.1,

DOI: 10.1021/acs.joc.5b02620
J. Org. Chem. 2016, 81, 662–666

141.1, 135.6, 133.7, 130.6, 130.0, 127.7, 126.0, 125.3, 20.8; HRMS (DART/TOF) m/z $[M + H]^+$ calcd for $C_{65}H_{51}$ 831.3985, found 831.3966. Anal. Calcd for $C_{65}H_{50}$·0.07$CHCl_3$: C, 93.08; H, 6.01; Cl, 0.90. Found: C, 92.91; H, 6.11; Cl, 0.93. A single crystal suitable for the X-ray diffraction study was obtained by slow diffusion of methanol into a chloroform solution of the sample.

1 (n = 5, R = 2′-m-xylyl): 78% yield (18.6 mg); mp >250 °C (not detected); T_d (onset) 463 °C (helium atmosphere); IR (powder) 2952 (w), 2920 (w), 1578 (w), 1483 (w), 1378 (w), 1318 (w), 1102 (w), 865 (s), 767 (s), 716 (s), 667 (m), 631 (w); ^{1}H NMR (400 MHz, $CDCl_3$) δ 8.74 (s, 5H), 7.52 (s, 10H), 7.21−7.13 (m, 15H), 2.15 (s, 30H); ^{13}C NMR (100 MHz, $CDCl_3$) δ 142.2, 141.9, 141.5, 136.2, 133.7, 127.5, 127.4, 125.0, 21.2; HRMS (DART/TOF) m/z $[M + H]^+$ calcd for $C_{70}H_{61}$ 901.4768, found 901.4761. Anal. Calcd for $C_{70}H_{60}$·0.41$CHCl_3$·0.52H_2O: C, 88.13; H, 6.46; Cl, 4.54. Found: C, 88.25; H, 6.86; Cl, 4.87. A single crystal suitable for X-ray diffraction studies was obtained by slow diffusion of methanol into the sample solution of dichloromethane.

1 (n = 6, R = 2′-tolyl): 81% yield (438 mg); mp >250 °C (not detected); T_d (onset) 509 °C (helium atmosphere); IR (powder) 1584 (m), 1489 (m), 1379 (m), 1219 (m), 864 (m), 770 (s), 726 (m), 713 (m), 667 (w), 626 (m) cm^{-1}; ^{1}H NMR (600 MHz, $CDCl_3$) δ 8.59 (t, J = 1.3 Hz, 6H), 7.76 (d, J = 1.3 Hz, 12H), 7.38 (d, J = 7.3 Hz, 6H), 7.33−7.30 (m, 18H), 2.39 (s, 18H); ^{13}C NMR (150 MHz, $CDCl_3$) δ 143.6, 141.8, 141.1, 135.6, 130.5, 129.9, 127.7, 126.6, 126.0, 125.9, 20.8; HRMS (APCI/TOF) m/z $[M + H]^+$ calcd for $C_{78}H_{61}$ 997.4768, found 997.4759. Anal. Calcd for $C_{78}H_{60}$·1.58$CHCl_3$·0.50H_2O: C, 79.99; H, 5.28; Cl, 14.06. Found: C, 79.76; H, 5.29; Cl, 13.80. A single crystal suitable for the X-ray diffraction study was obtained by slow diffusion of methanol into a chloroform solution of the sample.

1 (n = 6, R = 2′-m-xylyl): 96% yield (1.04 g); mp >250 °C (not detected); T_d (onset) 518 °C (helium atmosphere); IR (powder) 1584 (m), 1461 (m), 1378 (m), 862 (s), 765 (s), 716 (m), 648 (m), 553 (w) cm^{-1}; ^{1}H NMR (600 MHz, $CDCl_3$) δ 8.58 (t, J = 1.4 Hz, 6H), 7.50 (d, J = 1.4 Hz, 10H), 7.18 (t, J = 7.6 Hz, 6H), 7.12 (d, J = 7.6 Hz, 12H), 2.12 (s, 36H); ^{13}C NMR (150 MHz, $CDCl_3$) δ 142.8, 141.8, 141.6, 136.2, 127.5, 127.4, 126.4, 126.2, 21.2; HRMS (APCI/TOF) m/z $[M + H]^+$ calcd for $C_{84}H_{73}$ 1081.5707, found 1081.5690. Anal. Calcd for $C_{84}H_{72}$·0.03$CHCl_3$: C, 93.01; H, 6.69; Cl, 0.29. Found: C, 92.92; H, 6.70; Cl, 0.37.

Device Fabrications and Characterizations. Prior to the device fabrications, all the compounds were purified by sublimation using ALS Technology P-100. Devices were fabricated in a two-region configuration by sublimation of base material and the $Ir(ppy)_3$ emitter. Other fabrication protocols and characterization methods are identical to those reported in the literature.[1−3,7]

■ ASSOCIATED CONTENT

Supporting Information

The Supporting Information is available free of charge on the ACS Publications website at DOI: 10.1021/acs.joc.5b02620.

Analytical data, X-ray crystallographic analysis, theoretical calculations, device characteristics, and NMR spectra (PDF)

X-ray data (CIF)

■ AUTHOR INFORMATION

Corresponding Authors

*E-mail: satosota@m.tohoku.ac.jp.

*E-mail: isobe@m.tohoku.ac.jp.

Notes

The authors declare no competing financial interest.

■ ACKNOWLEDGMENTS

This work was partly supported KAKENHI (24241036, 25107708, 25102007). We thank Dr. M. Oinuma, Dr. S. Takahashi, Mr. H. Seki, and Ms. C. Yang (ERATO) for the large-scale preparation of [n]CMP, and Mr. H. Kiso (ERATO) for his technical assistance in the device fabrications.

■ REFERENCES

(1) Nakanishi, W.; Yoshioka, T.; Taka, H.; Xue, J. Y.; Kita, H.; Isobe, H. *Angew. Chem., Int. Ed.* **2011**, *50*, 5323−5326.

(2) Xue, J. Y.; Ikemoto, K.; Takahashi, N.; Izumi, T.; Taka, H.; Kita, H.; Sato, S.; Isobe, H. *J. Org. Chem.* **2014**, *79*, 9735−9739.

(3) Nakanishi, W.; Hitosugi, S.; Piskareva, A.; Shimada, Y.; Taka, H.; Kita, H.; Isobe, H. *Angew. Chem., Int. Ed.* **2010**, *49*, 7239−7242.

(4) Iyoda, M.; Yamakawa, J.; Rahman, M. J. *Angew. Chem., Int. Ed.* **2011**, *50*, 10522−10553.

(5) Silver, M.; Rho, J. R.; Olness, D.; Jarnagin, R. C. *J. Chem. Phys.* **1963**, *38*, 3030−3031.

(6) Hirth, H.; Stöckmann, F. *Phys. Status Solidi B* **1972**, *51*, 691−699.

(7) Xue, J. Y.; Izumi, T.; Yoshii, A.; Ikemoto, K.; Koretsune, T.; Akashi, R.; Arita, R.; Taka, H.; Kita, H.; Sato, S.; Isobe, H. *Chem. Sci.* **2015**, DOI: 10.1039/C5SC03807C.

(8) One example of a three-region single-layer OLED with the EQE value (EQE = 26.8%) higher than ours has been reported by using the multicomponent (donor−acceptor) base material: Hudson, Z. M.; Wang, Z.; Helander, M. G.; Lu, Z.-H.; Wang, S. *Adv. Mater.* **2012**, *24*, 2922−2928.

(9) For three-region single-layer OLEDs with EQE values over 10% using the multicomponent base material, see: (a) Cai, C.; Su, S.-J.; Chiba, T.; Sasabe, H.; Pu, Y.-J.; Nakayama, K.; Kido, J. *Org. Electron.* **2011**, *12*, 843−850. (b) Qiao, X.; Tao, Y.; Wang, Q.; Ma, D.; Yang, C.; Wang, L.; Qin, J.; Wang, F. *J. Appl. Phys.* **2010**, *108*, 034508.

(10) (a) Ishiyama, T.; Takagi, J.; Ishida, K.; Miyaura, N.; Anastasi, N. R.; Hartwig, J. F. *J. Am. Chem. Soc.* **2002**, *124*, 390−391. (b) Mkhalid, I. A. I.; Barnard, J. H.; Marder, T. B.; Murphy, J. M.; Hartwig, J. F. *Chem. Rev.* **2010**, *110*, 890−931. (c) Hartwig, J. F. *Chem. Soc. Rev.* **2011**, *40*, 1992−2002.

(11) (a) Hitosugi, S.; Nakamura, Y.; Matsuno, T.; Nakanishi, W.; Isobe, H. *Tetrahedron Lett.* **2012**, *53*, 1180−1182. (b) Matsuno, T.; Kamata, S.; Hitosugi, S.; Isobe, H. *Chem. Sci.* **2013**, *4*, 3179−3183. (c) Sun, Z.; Sarkar, P.; Suenaga, T.; Sato, S.; Isobe, H. *Angew. Chem., Int. Ed.* **2015**, *54*, 12800−12804.

(12) (a) Miyaura, N.; Yamada, K.; Suzuki, A. *Tetrahedron Lett.* **1979**, *20*, 3437−3440. (b) Miyaura, N.; Suzuki, A. *Chem. Rev.* **1995**, *95*, 2457−2483.

(13) The performances in PE and CE are convertible with the EQE performance, and considering the fundamental importance of EQE values to measure the electro-optical conversion, we consistently compare the raw EQE values in this study (see also ref 7).

(14) Smith, L. H.; Wasey, J. A. E.; Barnes, W. L. *Appl. Phys. Lett.* **2004**, *84*, 2986−2988.

(15) Pettersen, E. F.; Goddard, T. D.; Huang, C. C.; Couch, G. S.; Greenblatt, D. M.; Meng, E. C.; Ferrin, T. E. *J. Comput. Chem.* **2004**, *25*, 1605−1612.

(16) *CrystalClear-SM Expert 2.1 b29*; Rigaku Corporation: Tokyo, Japan, 2013.

(17) Altomare, A.; Cascarano, G.; Giacovazzo, C.; Guagliardi, A. *J. Appl. Crystallogr.* **1993**, *26*, 343−350.

(18) Palatinus, L.; Chapuis, G. *J. Appl. Crystallogr.* **2007**, *40*, 786−790.

(19) Sheldrick, G. M. *Acta Crystallogr., Sect. A: Found. Crystallogr.* **2008**, *A64*, 112−122.

(20) *CrystalStructure 4.1*; Rigaku Corporation: Tokyo, Japan, 2014.

(21) Kabuto, C.; Akine, S.; Nemoto, T.; Kwon, E. *Nippon Kessho Gakkaishi* **2009**, *51*, 218−224.

DOI: 10.1021/acs.joc.5b02620
J. Org. Chem. 2016, 81, 662−666